Unclassified

SECURITY CLASSIFICATION OF THIS PAGE

4

AD-A204 612

DTIC ELECTE FEB 21 1989 D

DTIC FILE COPY

REPORT DOCUMENTATION PAGE

1a. REPORT SECURITY CLASSIFICATION: Unclassified	1b. RESTRICTIVE MARKINGS
2a. SECURITY CLASSIFICATION AUTHORITY	3. DISTRIBUTION/AVAILABILITY OF REPORT: Unlimited. DISTRIBUTION STATEMENT A: Approved for public release; Distribution Unlimited
2b. DECLASSIFICATION/DOWNGRADING SCHEDULE	
4. PERFORMING ORGANIZATION REPORT NUMBER(S): Final Report	5. MONITORING ORGANIZATION REPORT NUMBER(S): Office of Naval Research
6a. NAME OF PERFORMING ORGANIZATION: Lehigh University, Bethlehem, PA 18015	6b. OFFICE SYMBOL (If applicable)
7a. NAME OF MONITORING ORGANIZATION: Office of Naval Research	
6c. ADDRESS (City, State and ZIP Code): Materials Research Center	7b. ADDRESS (City, State and ZIP Code): 800 North Quincy Street, Arlington, VA 22217
8a. NAME OF FUNDING/SPONSORING ORGANIZATION: Office of Naval Research	8b. OFFICE SYMBOL (If applicable)
9. PROCUREMENT INSTRUMENT IDENTIFICATION NUMBER: N00014-82-K-0050	
8c. ADDRESS (City, State and ZIP Code): 800 North Quincy Street, Arlington, VA 22217	10. SOURCE OF FUNDING NOS. PROGRAM ELEMENT NO. / PROJECT NO. / TASK NO. / WORK UNIT NO.
11. TITLE (Include Security Classification): PolyBEMO and Polyethers	
12. PERSONAL AUTHOR(S): J.J. Fay, C. J. Murphy, and L. H. Sperling	
13a. TYPE OF REPORT: Final	13b. TIME COVERED: FROM 1982 TO 1989
14. DATE OF REPORT (Yr., Mo., Day): January 22, 1989	15. PAGE COUNT: 35
16. SUPPLEMENTARY NOTATION	
17. COSATI CODES: FIELD / GROUP / SUB. GR.	18. SUBJECT TERMS (Continue on reverse if necessary and identify by block number): PolyBEMO, Melting behavior, morphology, crystal structure.

19. ABSTRACT (Continue on reverse if necessary and identify by block number)

Two crystalline melting peaks have been observed by differential scanning calorimetry for low molecular weight poly(3,3-bis-(ethoxymethyl) oxetane), polyBEMO, whereas only one melting peak has been observed for samples of higher molecular weight. Crystallization of low mol. wt. samples at large supercoolings produces the lower melting form, while low supercooling or annealing favors the higher melting species. Enthalpy of fusion values obtained by DSC for a multiple melting endotherm sample range from 28 to 39 j/g for crystallization temperatures from 58 to 35°C, respectively. Optical microscopy studies indicate that the lower melting peak corresponds to a spherulitic type of morphology and the higher melting peak correlates to a fine grained crystal structure. Wide angle X-ry powder diffraction studies do not detect differences in the crystal structures. (JF)

20. DISTRIBUTION/AVAILABILITY OF ABSTRACT: UNCLASSIFIED/UNLIMITED ☒ SAME AS RPT. ☐ DTIC USERS ☐	21. ABSTRACT SECURITY CLASSIFICATION: Unclassified
22a. NAME OF RESPONSIBLE INDIVIDUAL: Dr. Richard Miller	22b. TELEPHONE NUMBER (Include Area Code): (202) 696-4403 / 22c. OFFICE SYMBOL

DD FORM 1473, 83 APR — EDITION OF 1 JAN 73 IS OBSOLETE.

Unclassified

SECURITY CLASSIFICATION OF THIS PAGE

Multiple Endotherm Melting Behavior in Relation to the Morphology of Poly[3,3-bis(ethoxymethyl) oxetane]

J. J. Fay[1], C. J. Murphy[2] and L. H. Sperling[3]

Center for Polymer Science and Engineering
Materials Research Center
Whitaker Lab #5
Lehigh University
Bethlehem, PA 19015

[1] Department of Chemistry

[2]Permanent Address:
East Stroudsburg University
East Stroudsburg, PA 18301

[3]Department of Chemical Engineering

Acknowledgements

The Authors wish to thank the Office of Naval Research for support through Contract No. N00014-82-K-0050 and Mr G. E. Manser of Aerojet Strategic Propulsion Co., Sacramento, CA 95813, for synthesizing materials used in this study.

Submitted to the Journal of Applied Polymer Science

Abstract

Two crystalline melting peaks have been observed by differential scanning calorimetry for low molecular weight poly[3,3-bis(ethoxymethyl) oxetane], polyBEMO, samples, M_n < $1x10^4$ g/mol, whereas only one melting peak has been observed for samples of higher molecular weight, M_n > $1x10^4$ g/mol. Crystallization of low molecular weight samples at large supercoolings produces the lower melting form while low supercooling or annealing favors the higher melting species. Enthalpy of fusion values obtained by DSC for a multiple melting endotherm sample range from 28 to 39 J/g for crystallization temperatures from 58 to 35°C, respectively. Optical microscopy studies indicate that the lower melting peak corresponds to a spherulitic type morphology and the higher melting peak correlates to a fine grained crystal structure. Wide angle X-ray powder diffraction studies do not detect differences in the crystal structures of samples exhibiting either one or two melting peaks which suggests that the multiple melting phenomenon is due to differences in morphology rather than the presence of different crystal forms.

Introduction

Many semicrystalline polymers show multiple melting endotherms when analyzed by differential scanning calorimetry, DSC and other methods. Factors, such as the molecular weight polydispersity index, or crystallite size, or the presence of different crystalline forms, have been ascribed to account for this phenomenon (1). Since the properties of semicrystalline polymers are dependent not only on the chemical structure of the polymer but also on crystal morphology, which may be controlled by crystallization conditions, there has been considerable research in this area. Morphological maps, constructed by Mandelkern and coworkers, relate the molecular weight of a polymer and its crystallization temperature with observed gross morphologies such as spherulites or hedrites (2,3). The relationships between physical properties and crystal structure and morphology have been reviewed by Mandelkern (4). Additionally, the effect of melt history in semicrystalline polymers has also recently been reviewed (5).

Differences in polypropylene melt viscosity have been reported for identical samples of polypropylene crystallized from solutions of differing concentration. Melt spun filaments produced from these samples were found to have different crystallization behaviors and

physical properties (6). Poly(aryl-ether-ether-ketone), PEEK, exhibits local order in the amorphous phase when it is melted below its equilibrium melting temperature. The order is disrupted when the sample is heated above the equilibrium melting temperature (7).

The multiple melting endotherms observed in fibrillar polyethylene crystals were attributed to the melting of specific morphological elements (8) whereas annealing of samples with multiple fusion endotherms can result in the rearrangement of imperfect crystallites into a more ordered form (9). Bell et al. (10-12) investigated the multiple melting phenomenon in poly(ethylene terephthalate) and nylon 66 and found that in each material the two melting peaks could be converted to the other by judicious choice of annealing conditions.

The crystallization behavior of several polyoxetanes, first synthesized by Farthing in 1955 (13,14), has been reported in recent years with differences in crystallization due to the nature of side chain substituents (15-17). Polyoxetane is found to have only one melting endotherm whereas poly(3,3-dimethyl oxetane) and poly(3,3-diethyl oxetane) may exhibit two endothermal peaks, depending on crystallization temperature. Additionally, the unsymmetrically substituted poly(3-ethyl,3-methyl oxetane) is also

semicrystalline; however, only one crystal modification is observed by X-ray. Poly[3,3-bis(chloromethyl)oxetane] is also known to exist in more than one crystal modification with either one form or a mixture of forms being present, depending on thermal conditions (18,19).

This is the sixth paper in a series (20-24) regarding the study of homopolymers and block copolymers based on poly[3,3-bis(ethoxymethyl)oxetane], polyBEMO, and other novel polyethers (25). Jones et al. (20) examined the thermal decomposition behavior of polyBEMO and observed an endothermal process yielding a dimer related structure as the main degradation product. Hardenstine et al. (21) employed the Hoffman-Weeks extrapolation procedure (26) to determine the equilibrium melting temperature of polyBEMO and its relationship to the formation of supermolecular structure.

Murphy et al. (22) found that spherulites were formed if the polymer melt is heated above the Hoffman-Weeks melting temperature, then cooled, while a fine structure results if the melt is always held below the Hoffman-Weeks melting temperature. The reason for this is unknown.

The viscoelastic behavior of polyBEMO block copolymers was investigated by Hardenstine et al. (23) whereas Murphy et al. (24) determined the values of k

and a in the Mark-Houwink equation for polyBEMO.

The phenomenon of multiple melting peaks was initially observed for polyBEMO by Hardenstine et al. (21) and then by Murphy et al. (24). In both studies, multiple melting phenomena were observed only for samples crystallized from the polymerization vessel, not for samples crystallized from the melt or from solution. In the present paper, the presence of multiple melting peaks in polyBEMO samples crystallized from the melt is characterized.

Experimental

Materials

PolyBEMO and poly[3,3-bis(chloromethyl) oxetane], polyBCMO structures are given in Table I. The synthesis of polyBEMO has been described previously (20,23). Samples were obtained from Mr. Gerry Manser of Aerojet Strategic Propulsion Co., Sacramento, CA. PolyBCMO was obtained from BDH Ltd. PolyBCMO was purified by precipitation from Fisher reagent grade ortho-dichlorobenzene. PolyBEMO samples were dried in a vacuum oven at 100°C until constant weight was obtained.

Differential Scanning Calorimetry

Thermal measurements utilized a Mettler TA3000 DSC30 Differential Scanning Calorimeter calibrated with indium (T_m = 156°C), lead(T_m = 327°C) and zinc (T_m = 419°C) standards obtained from Mettler. Polymer samples of approximately 5-15 mg were placed in tared aluminum pans, weighed on a Perkin-Elmer Autobalance AD-1 and sealed. The sample cell was purged with nitrogen at a flow rate of 200 mL/min and was cooled with liquid nitrogen. Heating and cooling rates of 1, 5, 10 and 20°C were used. Typically, a 10 mg sample was heated at 20°C/min to a temperature above the Hoffman-Weeks melting temperature and held isothermally for ten minutes to remove any previous thermal history. The

sample was then cooled at 20°C/min to crystallize isothermally at a specified temperature and then evaluated at a heating rate of 1°C/min. The three steps were linked together to form a continuous thermal analysis program.

Optical Microscopy

A Zeiss 20-T microscope equipped with reflecting and transmitting polarized-light Nomarski optics, a Zeiss M-35 automatic exposure control camera, and a LinKam TH600 hotstage was used to observe melting points and crystalline morphology. The microprocessor controlled hot-stage, calibrated with benzoic acid (T_m = 122°C), is programmable for heating and cooling at rates of 0.1 to 90°C in the range of -180 to +500°C with maximum temperature control of 0.1°C. The hotstage may also be held isothermally for extended periods of time within the above range. Kodacolor VR ISO 1000 film was used.

X-ray Diffraction

X-ray powdered diffraction studies were done on a Phillips APD 3720 automated X-ray powder diffractometer with a copper target and a Phillips XRG X-ray generating Unit. A nickel filter was used to isolate the Cu kα line (λ =1.542Å). A scan rate of 1°/min with 0.02°increments was used.

Molecular Weight Determination

Molecular weight distributions were estimated using a Waters gel permeation chromatograph (GPC) calibrated with polystyrene standards using tetrahydrofuran as solvent.

Results and Discussion

The molecular weight distribution of the polyBEMO samples is summarized in Table II. The polydispersity of the samples is approximately M_w/M_n=2.5 and there is a small low molecular weight peak present in all samples.

Hoffman-Weeks Melting Temperatures

The morphology of single melting endotherm polyBEMO samples may be controlled by varying the thermal history of the sample. When it is heated to a melt liquid temperature, T_l, above the Hoffman-Weeks equilibrium melting temperature, T_m^*, spherulites form upon crystallization. Non-spherulitic morphologies are usually obtained when the melt liquid temperature remains below T_m^* (22).

The effect of crystallization temperature on the melting temperature of polyBEMO is illustrated in Figure 1. As the crystallization temperature of the sample is decreased, there is a corresponding decrease in the observed melting temperature and a small decrease in the heat of fusion from 43 J/g at T_c = 65°C to 40 J/g at T_c = 35°C. This may only indicate a slight reduction in the fraction of crystallized material. The specific enthalpy of fusion for the crystalline phase of polyBEMO is 54 J/g (21). In Figure 2, plotting both the peak temperature and the temperature at which the DSC curve

returns to the baseline results in equilibrium melting temperatures of 94 and 105°C, respectively. The value of T_m^* obtained by the peak temperature corresponds to the value of 92°C obtained previously by optical microscopy, which permits a closer approach to equilibrium conditions (22). The heating rate could be varied over a wide range without appreciably affecting the melting behavior of the sample as evidenced by the constant peak temperatures and an enthalpy of fusion of 40 J/g in each case, Figure 3. Various thermal history regimes were applied on the sample, however, no additional melting peaks were observed.

Multiple Melting Temperatures

Samples of polyBEMO have previously been found by differential scanning calorimetry to exhibit two melting peaks (21). However, multiple melting peaks have not been previously observed for samples crystallized from the melt, as is the case for the present study. The position and magnitude of the endotherms obtained in multiple melting samples are very dependent upon the thermal history of the sample. Sample #2 was heated to a melt liquid temperature, T_l, of 100°C, which is above the Hoffman-Weeks melting temperature determined for higher molecular weight samples by optical microscopy, and crystallized isothermally at various temperatures within the DSC. Evaluation of the samples at a heating

rate of 1°C/min resulted in the melting behavior depicted in Figure 4. At the lowest crystallization temperature, T_c=35°C, two melting peaks are observed. As T_c is increased there is a shift in the low temperature peak to higher values and a decrease in the size of the high temperature peak. There is also a corresponding decrease in the total heat of fusion for both peaks with higher values of T_c, see Table III. Comparatively, the heat of fusion changes only slightly with changes in the crystallization temperature for the single endotherm sample shown in Figure 1. The DSC data suggests that at higher crystallization temperatures only one melting peak will be observed.

Whereas a unique value for T_m^* was determined for single endotherm polyBEMO samples, it appears from Figure 4 that the procedure to determine the Hoffman-Weeks equilibrium melting temperature is not applicable to samples which exhibit multiple melting peaks. The relatively constant position of the high temperature peak at high values of T_c renders the Hoffman-Weeks extrapolation procedure ineffective. This finding has not been previously reported.

The high temperature melting peak appears to be due to the simultaneous melting and recrystallization during evaluation in the DSC. Ikeda (27) proposed that the lack of an observable crystallization exotherm may result

when the melting endotherm and the recrystallization exotherm cancel. This may explain why an exotherm is not observed for the polyBEMO samples. The effect of heating rate on sample #2, crystallized at 35°C is shown in Figure 5. At slow heating rates considerable recrystallization occurs resulting in a larger high temperature peak and total heat of fusion as compared to conditions of more rapid heating rates. Heat of fusion values for the samples in Figure 5 are listed in Table IV. The recrystallized material melts at about the same temperature, regardless of heating rate, as indicated by the constant value of the peak temperature.

The recrystallization process becomes more evident when the sample is held isothermally just above the low temperature melting peak and is then crystallized at 35°C. In Figure 6, the dotted curve represents the melting behavior obtained when the sample is crystallized from the melt at 35°C and evaluated at 1°C/min. The dashed curve is for a similarly crystallized sample which was annealed at 68°C, crystallized at 35°C, and then evaluated. The heat of fusion for the sample annealed at 68°C is 27 J/g compared to the value of 39 J/g obtained for the sample crystallized at 35°C. Annealing at 68°C may result in a lower overall degree of crystallinity. The disappearance of the low temperature melting peak from

the latter curve indicates that annealing at high temperatures favors the formation of the higher melting species.

Optical microscopy of sample #3 treated under similar conditions reveals changes in morphology acompanying the transitions detected by DSC. When the sample was crystallized at 35°C from a melt liquid temperature of 100°C, a spherulitic morphology was observed, Figure 7a. Two melting peaks, at 65 and 73°C, are observed by DSC for a similarly treated sample. As the temperature of the sample is increased at 5°C/min to 68°C, which is just above the lower endotherm, the spherulitic structure dissipates and a fine grained morphology remains, Figure 7b. Cooling the sample results in crystallization, which apparently is confined to the domains of the original spherulites, see Figure 7c. Under these conditions a nonspherulitic crystallization is expected on the basis of the melt liquid temperature being below T_m^*. Subsequent analysis shows that there is an indication of the previous structure in the DSC curve, which may be attributed to incomplete melting, however, the low melting material is converted to the higher temperature material by annealing at temperatures above the melting point of the lower melting species.

X-ray diffraction studies of the as received

polyBEMO sample, Figure 8a, reveals additional peaks that are not present in samples crystallized from the melt at different conditions, Figure 8b. Samples crystallized at 35 and 60°C, which exhibit different melting behaviors as observed by DSC, have identical X-ray diffraction patterns, of the type shown in Figure 8b, which suggests that the multiple melting phenomenon is due to differences in crystallite arrangement, not to the presence of two different crystal lattices. Small quantities of catalyst or other material that might have acted as a heterogeneous nucleating agent during the original recrystallization may be ineffective nucleating agents in the melt. They may also have been too dilute in subsequent solution recrystallizations by Hardenstine et al. (21) to induce crystallization. The explanation for the additional peaks observed in the X-ray diffraction patterns for the as received material is still unknown.

PolyBCMO shows multiple melting endotherms which may be attributed to the ability of polyBCMO to crystallize in two crystal forms, depending on the thermal history of the sample. These crystal forms have been identified by X-ray diffraction techniques (19). PolyBCMO slowly cooled from the melt results in the α-crystal form which has a higher melting temperature than the β-form, which is obtained by quenching the

sample and then annealing above the glass transition temperature of the polymer (T_g = 7°C). As is shown in Figure 9, crystallization at relatively small supercoolings results in a large melting endotherm at 170°C accompanied by a much smaller endotherm at a lower temperature. Crystallization at larger supercoolings results in the observation of three melting endotherms with the highest temperature peak being found at slightly lower temperature than in the higher crystallization case. Note that when T_c = 35 and 100°C, the melting peak positions remain constant even though there are changes in peak size. There is a slight overall decrease in the heat of fusion observed with increasing crystallization temperature, Table V, which may be attributed to incomplete crystallization or diminished recrystallization during the heating cycle.

It is of interest to note that the polyBEMO samples that exhibit multiple melting phenomenon all have lower molecular weights than the single endotherm samples. This suggests that low molecular weight might be a contributing factor in the formation of a kinetically favored morphology versus a higher melting, thermodynamically favored morphological structure. Apparently, the low molecular weight material present in all of the samples, as evidenced by the low molecular weight peak in the GPC trace, does not contribute to the

multiple melting phenomenon. The ether oxygen located in the polyBEMO backbone provides a great deal of flexibility to the polymer. Little is known about the origin of the liquid crystalline phase in flexible polymers such as the polysiloxanes (28). Whether or not polyBEMO can exhibit similar liquid crystal behavior is still to be determined.

Conclusions

The phenomenon of multiple melting peaks observed for polyBEMO samples comes to the fore for when the molecular weight is less than $M_n = 1x10^4$ g/mol. The Hoffman-Weeks extrapolation procedure to determine the equilibrium melting temperature is not applicable in the case of multiple endotherm polyBEMO samples because of the relatively constant melting temperature of the high temperature endotherm. Wide angle X-ray powder diffraction does not detect differences in the crystal structure of samples containing either one or two melting peaks which indicates that there is only one crystalline form present. Optical microscopy studies reveal that the lower melting peak corresponds to a spherulitic morphology and the higher melting peak correlates to a fine-grained, non-spherulitic morphology. Therefore, it is concluded that the multiple melting peaks observed by DSC are due primarily to differences in crystallite arrangement and size, not to two crystal lattices.

References

1. M. C. Lang, C. Noel and A. P. Legrand, J. Polym. Sci., Polym. Phys. Ed., 15, 1319 (1977).

2. I. G. Voight-Martin and L. Mandelkern, J. Polym. Sci., Polym. Phys. Ed., 19, 1769 (1981).

3. R. C. Allen and L. Mandelkern, J. Polym. Sci., Polym. Phys. Ed., 20, 1465 (1982).

4. L. Mandelkern, in "Physical Properties of Polymers", J. E. Mark, A. Eisenberg, W. W. Graessley, L. Mandelkern and J. L. Koenig, eds., American Chemical Society, Washington, 1984.

5. J. Rault, CRC Crit. Rev. Solid State Mat. Sci., 13(1), 57 (1986).

6. K. Koyama and O. Ishizuka, Polym. J. 12, 735 (1980).

7. H. X. Nguyen and H. Ishida, Polymer, 27, 1400 (1986).

8. A. J. Pennings and A. Zwijnenburg, J. Polym. Sci., Polym. Phys. Ed., 17, 1011 (1979).

9. R. C. Roberts, Polymer, 10, 117 (1969).

10. J. P. Bell, P. E. Slade and J. H. Dumbleton, J. Polym. Sci., Pt. A-2, 6, 1773 (1968).

11. J. P. Bell and J. H. Dumbleton, J. Polym. Sci., Pt. A-2, 1033 (1969).

12. J. P. Bell and T. Murayama, J. Polym. Sci., Pt. A-2, 1059, (1969).

13. A. C. Farthing, J. Chem. Soc., 3648 (1955).

14. A. C. Farthing, J. Appl. Chem., 8, 186 (1958).

15. E. Perez, M. A. Gomez, A. Bello and J. G. Fatou, Coll. Polym. Sci., 261, 571 (1983).

16. M. A. Gomez, E. Perez, A. Bello and J. G. Fatou, Polym. Commun., 27 166 (1986).

17. M. A. Gomez, J. G. Fatou and A. Bello, Eur. Polym. J., 22(8), 661 (1982).

18. J. Brandrup and E. H. Immergut, "Polymer Handbook", Wiley-Interscience, New York, III-42, 1975.

19. D. J. H. Sandiford, J. Appl. Chem., 8, 188 (1958).

20. R. B. Jones, C. J. Murphy, L. H. Sperling, M. Farber, S. P. Harris and G. E. Manser, J. Appl. Polym. Sci., 30, 95 (1985).

21. K. E. Hardenstine, G. V. S. Henderson, L. H. Sperling, C. J. Murphy and G. E. Manser, J. Polym. Sci., Polym, Phys. Ed., 23, 1597 (1985).

22. C. J. Murphy, G. V. S. Henderson, E. A. Murphy and L. H. Sperling, Polym. Sci. Eng., 27, 781 (1987).

23. K. E. Hardenstine, C. J. Murphy, R. B. Jones, L. H. Sperling and G. E. Manser, J. Appl. Polym. Sci., 30, 2051 (1985).

24. E. A. Murphy, T. Ntozakhe, C. J. Murphy, J. J. Fay and L. H. Sperling, J. Appl. Polym. Sci., accepted.

25. G. E. Manser (Thiokol), U.S. Patent 4,393,199 (1983).

26. J. D. Hoffman and J. J. Weeks, J. Res. Natl. Bur. Stand., 66A, 13 (1962).

27. M. Ikeda, Kobunshi Kagaku, 25, 87 (1968).

28. N. A. Plate and V. P. Shibaev, "Comb-Shaped Polymers and Liquid Crystals", Plenum Press, New York, (1987).

List of Tables

Table I. Structures of polymers.

Polymer	Abbreviation	Structure
poly[3,3–bis(ethoxymethyl) oxetane]	poly(BEMO)	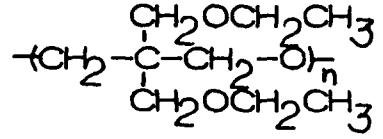
poly[3,3–bis(chloromethyl) oxetane]	poly(BCMO)	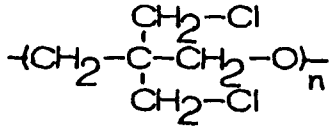

Table II.

Molecular weight analysis of poly(BEMO) samples

Sample	Mn	Mw	Mw/Mn
1	14,600	36,700	2.5
* 2	6,500	17,000	2.6
* 3	7,500	17,900	2.4
* 4	8,400	23,800	2.8
5	16,400	42,900	2.6

*multiple melting peaks observed.

Table III. Effect of crystallization temperature on the heat of fusion of polyBEMO sample #2.

Tc (°C)	ΔH_f (J/g)
57.5	28
55	31
45	37
35	39

Table IV. Effect of heating rate on the heat of fusion of polyBEMO sample #2.

Heating rate (°C/min)	ΔH_f (J/g)	Tm (°C)
1	39	76
5	36	73
10	33	73

Table V. Effect of crystallization temperature on the heat of fusion of polyBCMO.

Tc (°C)	ΔH_f (J/g)
125	36
100	38
35	46

List of Figures

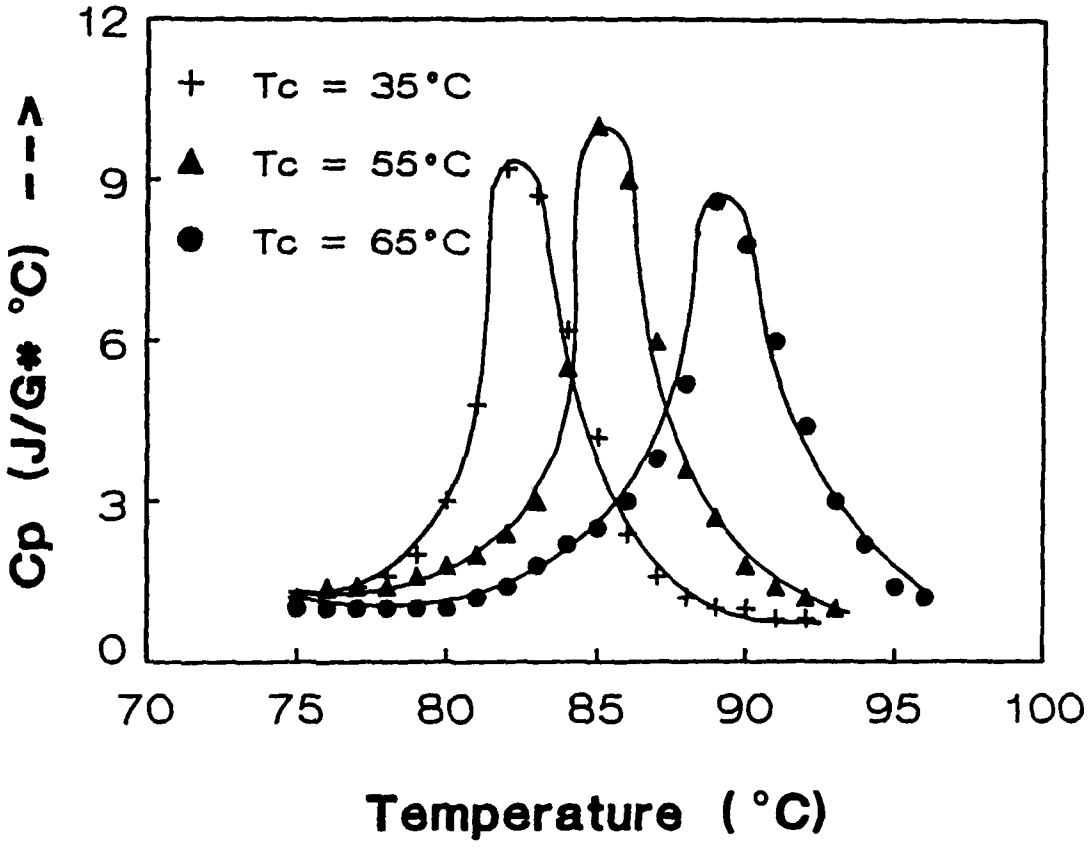
12
9
6
3
0
Cp (J/G* °C) --->
+ Tc = 35°C
▲ Tc = 55°C
● Tc = 65°C
70
75
80
85
90
95
100
Temperature (°C)

Figure 1.

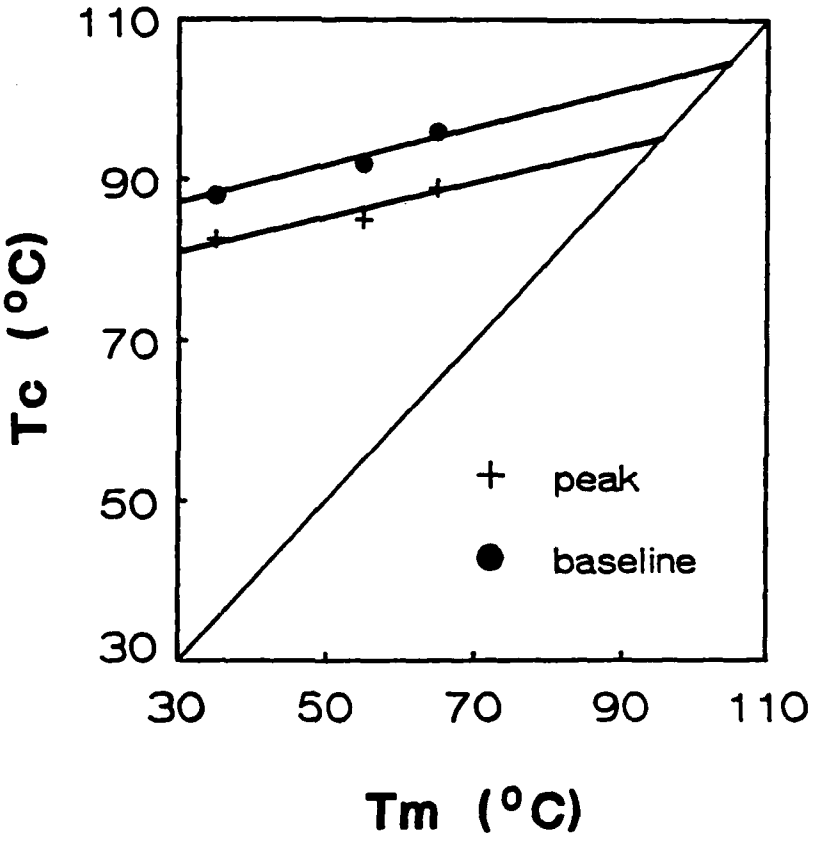

Figure 2.

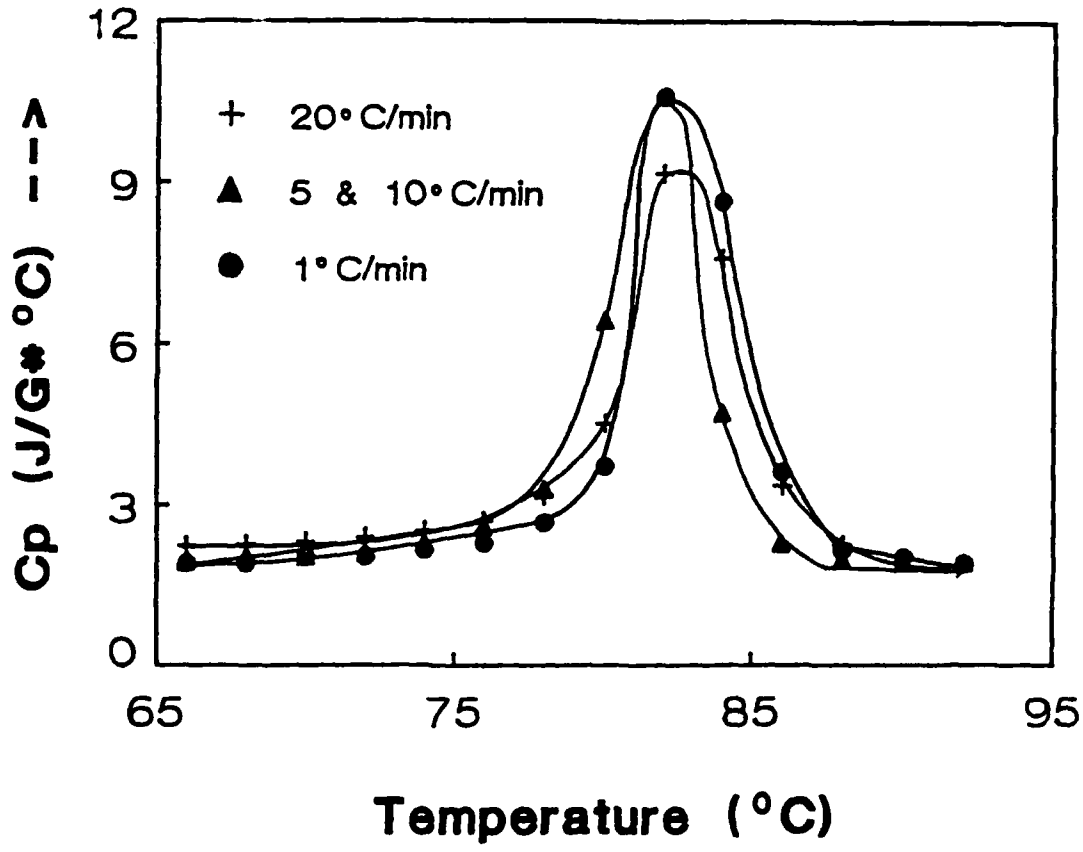

Figure 3.

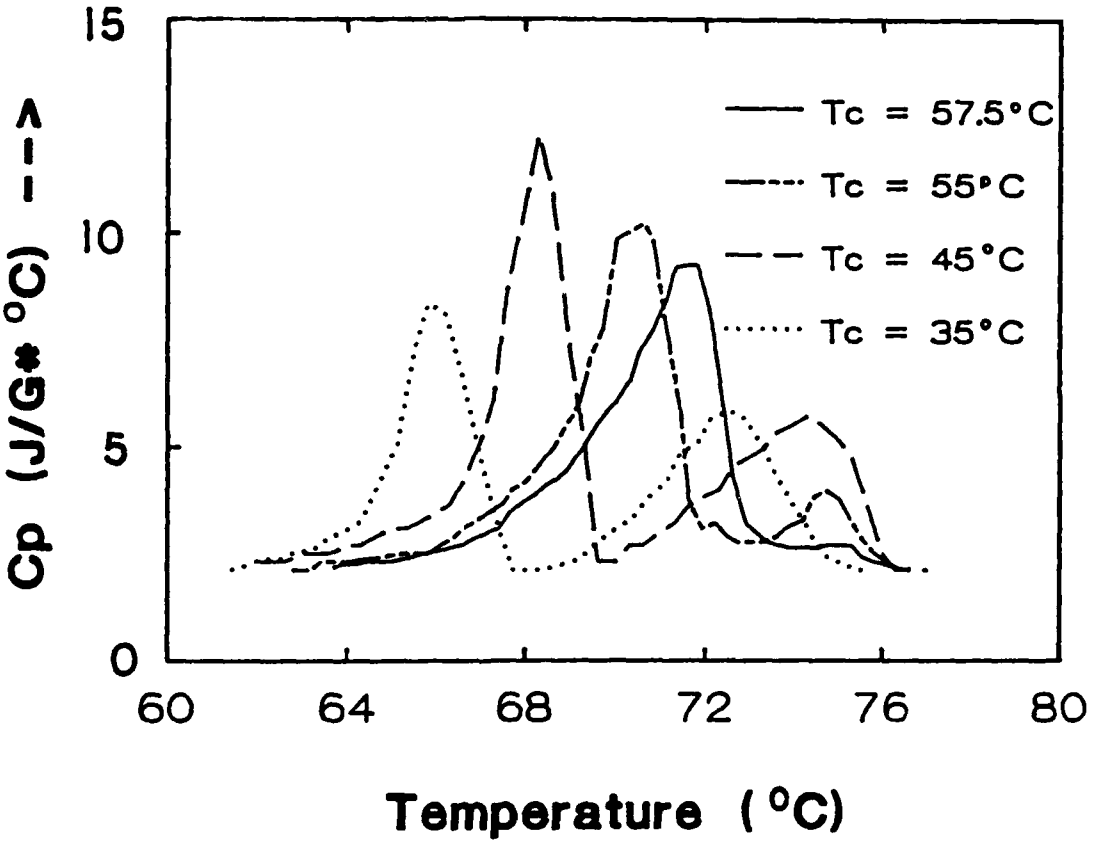
15
10
5
0
60
64
68
72
76
80
Cp (J/G* °C) --->
Temperature (°C)
Tc = 57.5°C
Tc = 55°C
Tc = 45°C
Tc = 35°C

Figure 4.

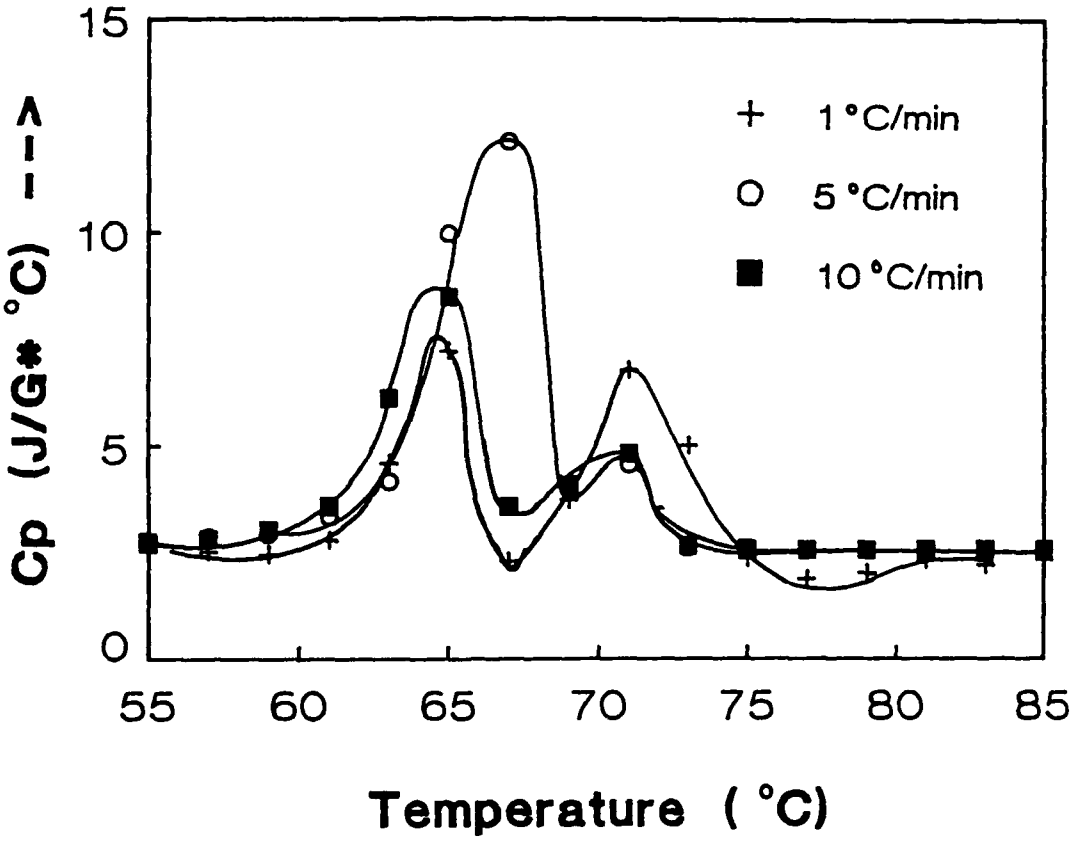
15
10
5
0
Cp (J/G* °C)
1 °C/min
5 °C/min
10 °C/min
55
60
65
70
75
80
85
Temperature (°C)

Figure 5.

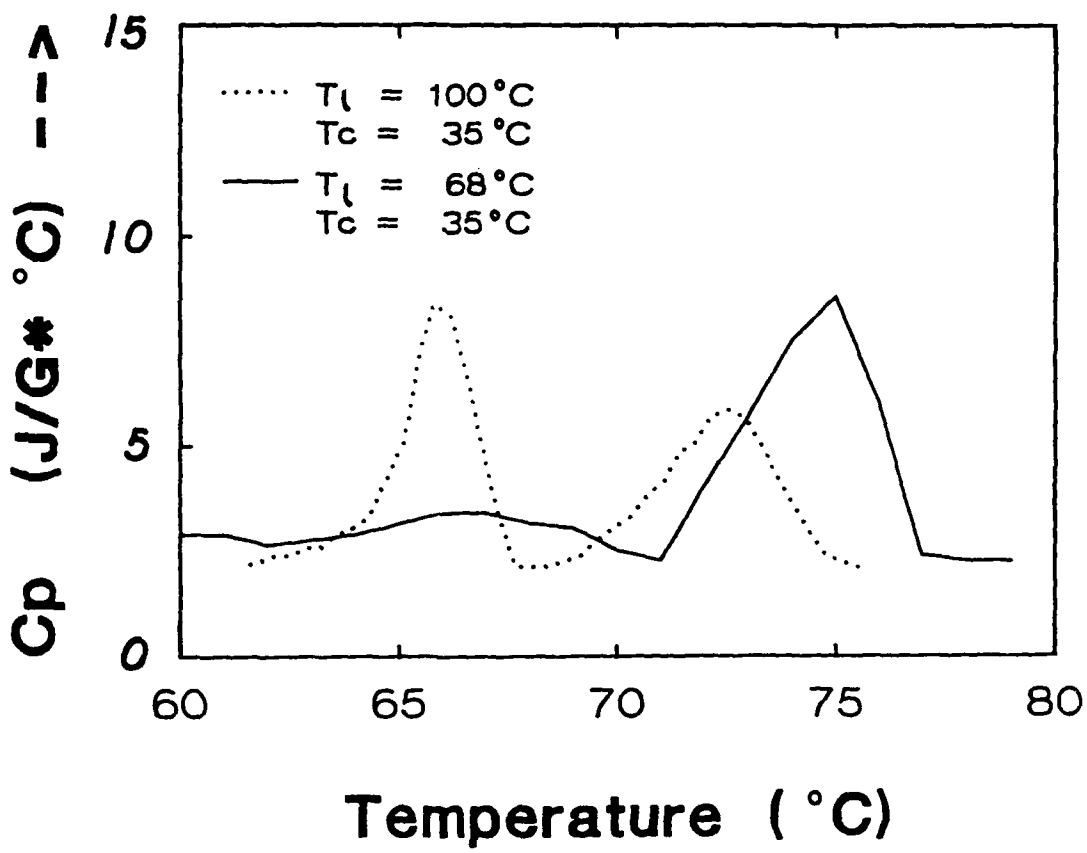
Cp (J/G* °C)
15
10
5
0
60
65
70
75
80
Tl = 100°C
Tc = 35°C
Tl = 68°C
Tc = 35°C
Temperature (°C)

Figure 6.

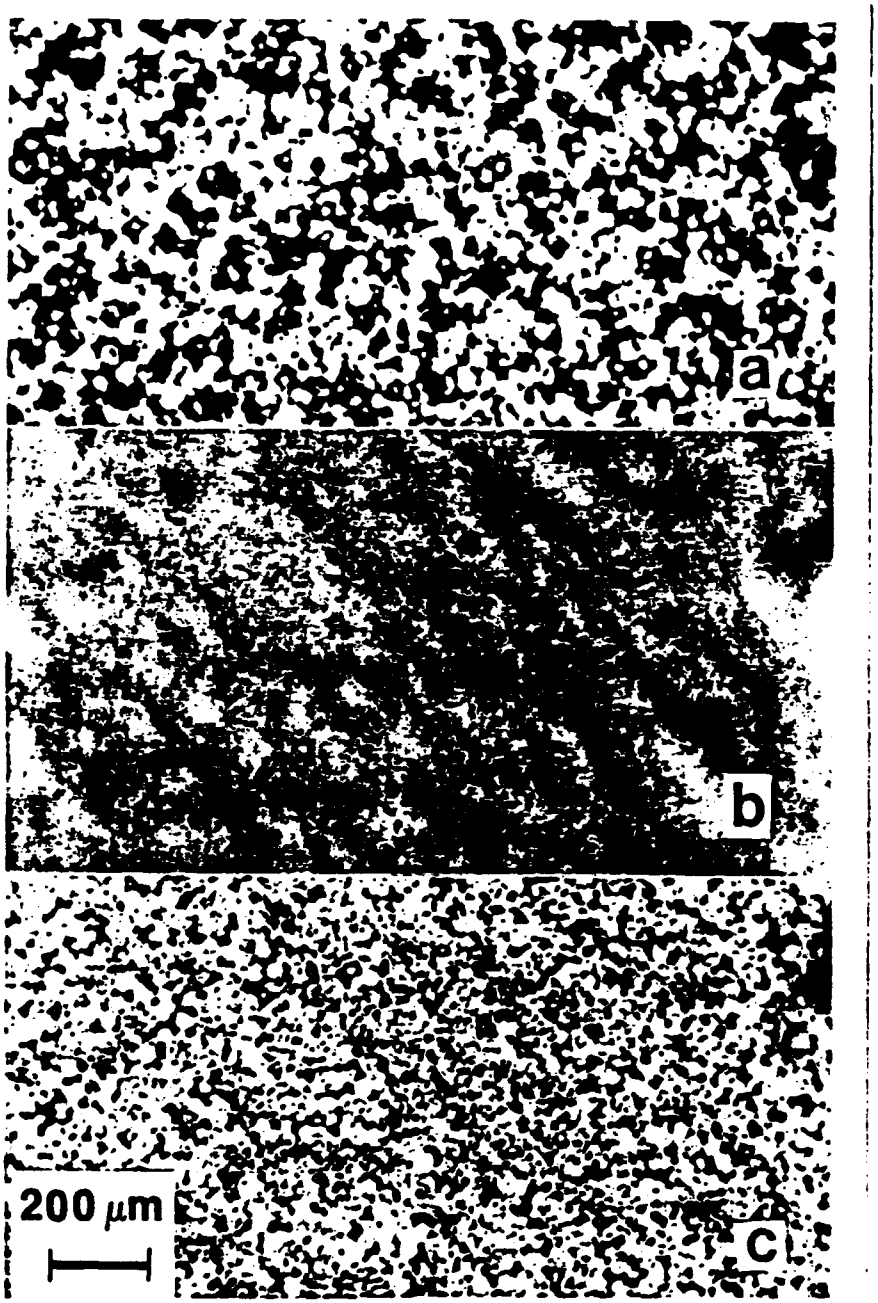

Figure 7.

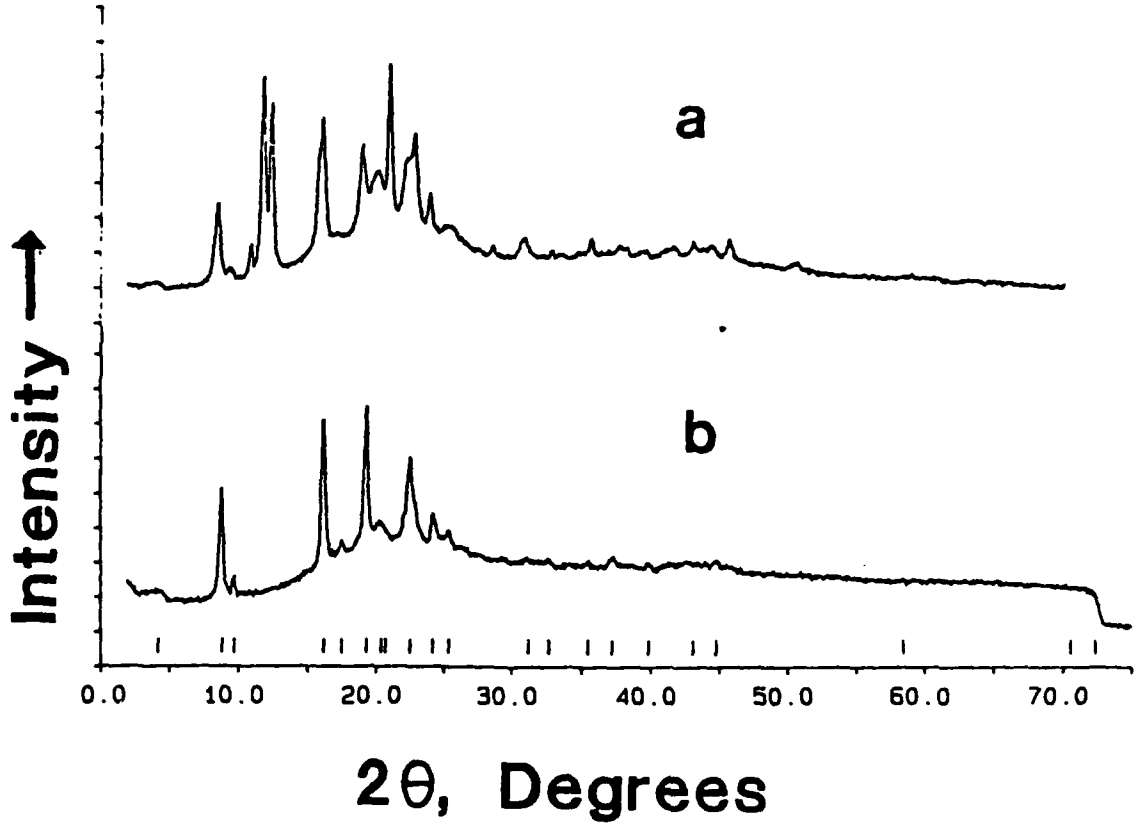

Figure 8.

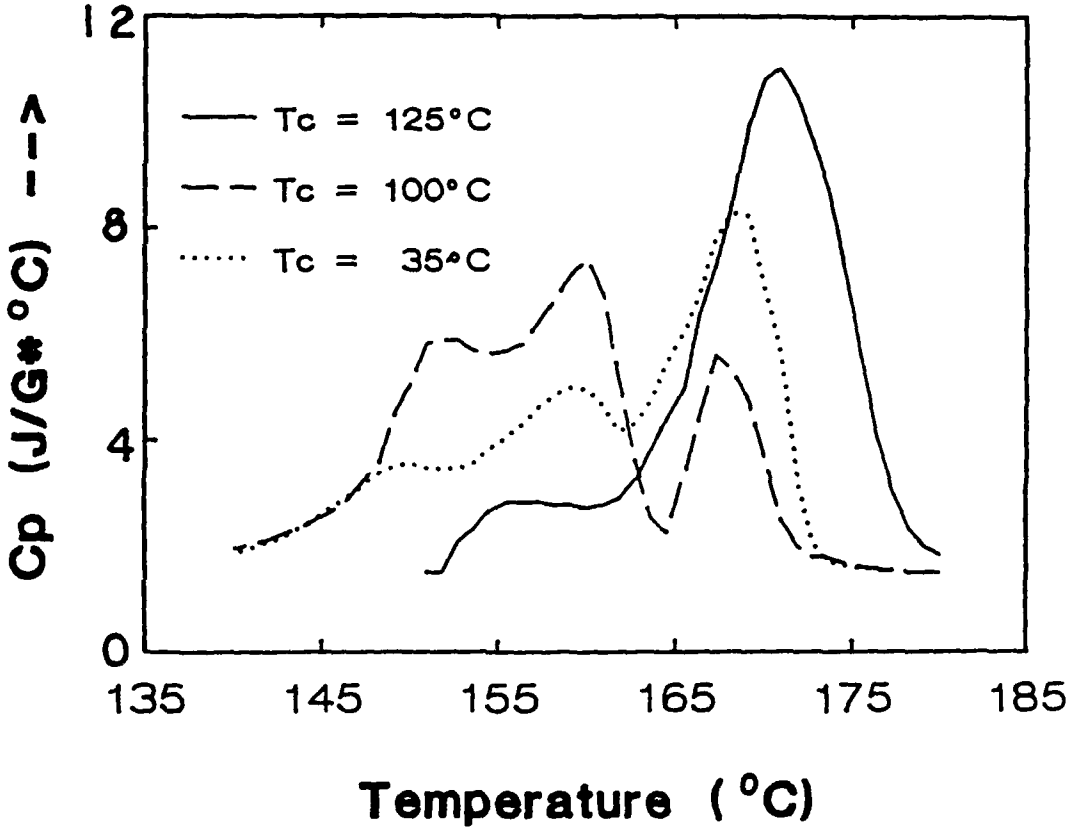
12
8
4
0
Cp (J/G* °C) --->
Tc = 125°C
Tc = 100°C
Tc = 35°C
135
145
155
165
175
185
Temperature (°C)

Figure 9.